Fuel Processing Technology 92 (2011) 2061–2067

Contents lists available at ScienceDirect

Fuel Processing Technology

journal homepage: www.elsevier.com/locate/fuproc

# Solid oxide derived from waste shells of *Turbonilla striatula* as a renewable catalyst for biodiesel production

Jutika Boro [a,*], Ashim J. Thakur [b], Dhanapati Deka [a]

[a] Department of Energy, Tezpur University, Napaam, Tezpur-784028, India
[b] Department of Chemical Sciences, Tezpur University, Tezpur-784028, India

ARTICLE INFO

*Article history:*
Received 1 November 2010
Received in revised form 24 May 2011
Accepted 6 June 2011
Available online 28 June 2011

*Keywords:*
Biodiesel
Transesterification
Solid oxide catalyst
Waste shell
Catalyst characterization

ABSTRACT

Biodiesel production via transesterification of mustard oil with methanol using solid oxide catalyst derived from waste shell of *Turbonilla striatula* was investigated. The shells were calcined at different temperatures for 4 h and catalyst characterizations were carried out by X-ray diffraction (XRD), scanning electron microscope (SEM), energy dispersive spectrometer (EDS), Fourier transform infrared spectrometer (FT-IR), thermogravimetric analysis (TGA)/differential scanning calorimetry (DSC) and Brunauer–Emmett–Teller (BET) surface area measurements . Formation of solid oxide i.e. CaO was confirmed at calcination temperature of 800 °C. The effect of the molar ratio of methanol to oil, the reaction temperature, catalyst calcination temperature and catalyst amount used for transesterification were studied to optimize the reaction conditions. Biodiesel yield of 93.3% was achieved when transesterification was carried out at 65 ± 5 °C by employing 3.0 wt.% catalyst and 9:1 methanol to oil molar ratio. BET surface area indicated that the shells calcined in the temperature range of 700 °C–900 °C exhibited enhanced surface area and higher pore volume than the shells calcined at 600 °C. Reusability of the catalysts prepared in different temperatures was also investigated.



## 1. Introduction

Increasing crude oil prices and environmental concerns have resulted in the search for alternative fuels. In developed countries there is a growing trend towards employing modern technologies and efficient bio-energy conversion using a range of biofuels, which are becoming cost-wise competitive with fossil fuels [1]. In this respect, biodiesel (fatty acid methyl esters) derived from the transesterification of vegetable oils or animal fats with methanol is a potential substitute for petroleum-based diesel fuels, due to its nontoxic, sulfur- and aromatic-free, biodegradable, and renewable features [2,3].

Biodiesel is comprised of monoalkyl esters of long chain fatty acids derived from vegetable oils or animal fats. Chemically, the vegetable oils and animal fats are complex mixtures of triglycerides and other minor components, such as free fatty acids, gums, waxes, etc. Though vegetable oils are a renewable and potentially inexhaustible source of energy with energy content close to diesel fuel, it cannot be used directly as fuel in diesel engine due to its high viscosity and free fatty acid content as well as gum formation [4,5]. There are a number of ways to reduce vegetable oils' viscosity. Dilution, microemulsification, pyrolysis, and transesterification are the four techniques applied to solve the problems encountered with high fuel viscosity. Out of these four methods, transesterification is the most viable process adopted known so far for the lowering of viscosity [6]. Transesterification of triglycerides with alcohol in the presence of catalyst can produce a new ester called biodiesel which can be effectively used as substitute for petroleum diesel in pure form or as blend [7]. It consists of a sequence of three consecutive reversible reactions. The first step is the conversion of triglycerides to diglycerides, followed by the conversion of diglycerides to monoglycerides, and finally monoglycerides into glycerol, yielding one ester molecule from each glyceride at each step [8]. Generally transesterification is carried out in the presence of a homogeneous or heterogeneous catalyst. Even though homogeneous catalyzed biodiesel production processes are relatively faster and show high conversions with minimal side reactions, they are still not very cost competitive with petrodiesel [9]. Besides, the catalyst cannot be recovered and must be neutralized and separated from the methyl ester phase at the end of the reaction, with the consequent generation of a large volume of wastewater. Conventional homogeneous catalysts are expected to be replaced by heterogeneous catalysts mainly in the near future because of environmental constraints and simplifications in the existing processes [10]. Heterogeneous catalysts could be easily separated from the reaction mixture by filtration and then reused. Use of solid catalysts instead of homogeneous catalysts could potentially lead to cheaper production costs and opportunities to operate in a fixed bed continuous process as illustrated by Feng et al. [11].

Some of the heterogeneous catalysts reported include calcium ethoxide [12], $CaTiO_3$, $CaMnO_3$, $Ca_2Fe_2O_5$, $CaZrO_3$, and $CaO–CeO_2$[13],

* Corresponding author. Tel.: +91 9864664257; fax: +91 3712 267005 6.
*E-mail address:* borojutikas@gmail.com (J. Boro).

0378-3820/$ – see front matter © 2011 Elsevier B.V. All rights reserved.
doi:10.1016/j.fuproc.2011.06.008

KF/hydrotalcite [14], sulfated zirconia [15], MgO, CaO, PbO, $PbO_2$, $Pb_3O_4$, $T_{l2}O_3$, and ZnO [16], heteropoly acids [17], MgO loaded with KOH [18], etc. Though all the catalysts mentioned above showed a comparative biodiesel yield,sulfated zirconia was found to be the best one. It was reported that 98.6% of yield was obtained with sulfated zirconia while the lowest yield of 85% was obtained with KF/hydrotalcite. It has been observed that the activities exhibited by the heterogeneous catalysts are very high but their synthesis routes are very lengthy and time consuming. Therefore, there is a need to search for an ideal heterogeneous catalyst which is low cost, ecofriendly in nature and exhibits high catalytic activity during transesterification.

To address these issues, catalyst research for the production of biodiesel is focused towards green catalyst. Such novel catalyst could be prepared either from biomass or from waste generated in the households. Recently waste shells of egg, oyster and shrimp were used for biodiesel production via transesterification. Nakatani et al. [19] reported a high biodiesel yield of 73.8% when the transesterification was catalyzed by combusted oyster shells and it could be reused for biodiesel production. In another experiment the viability of waste chicken egg shells as solid catalyst was investigated by Wei et al. [20] for transesterification. The researchers not only obtained a high biodiesel yield but they also emphasized that the catalyst prepared was environmentally benign and could be reused.

In this work, we have carried out transesterification using the waste shells of *Turbonilla striatula* as catalyst. It is easily available in Chirang district of Assam, India and is widely distributed in swamp areas, rivers and agricultural fields. Meat remaining inside the shell is used as one of the food items by some groups of people in that locality. After taking out the meat, the shells have no practical use and are thrown out as waste materials. The activated waste shells are mainly composed of CaO and can be used as heterogeneous catalyst, consequently adding value to the waste generated. In addition, the synthesis route reported here has benefits over existing technologies because this method of preparing catalyst is simple, inexpensive, environmentally benign as well as a good catalyst for biodiesel production. Moreover the utilization of such catalysts for the production of biodiesel also provides an alternative for sustainable development to economically weaker nations. Therefore, the shells of *T. striatula* may present a good option as a renewable catalyst for biodiesel production. In this study, along with the physical and chemical characterizations of the catalyst, biodiesel components were also analyzed. The effect of various reaction conditions on the biodiesel yields was also investigated.

## 2. Materials and methods

### 2.1. Materials and catalyst preparation

Waste shells of *T. striatula* were obtained from a local household of Chirang district of Assam, India. Synthesis-grade methanol (≥99% assay and ≤0.2% water content) was purchased from Merck Limited, Mumbai, India and was used as received. Commercial edible-grade mustard oil was purchased from the market and used without further purification. The shell was washed with distilled water several times to remove any organic impurity attached to it and then allowed to dry in an oven at a temperature of 120 °C for 24 h. After drying, the shell was crushed using a pestle and mortar followed by grinding in a grinder machine till it became powdered. It was then allowed to pass through a 0.8 mm sieve mesh. The powdered shell was then calcined at a different temperature range of 600 to 900 °C for 4 h and then stored in a desiccator.

### 2.2. Reaction procedures

Transesterification was carried out in laboratory scale in a 250 mL round bottom two neck flask equipped with a water cooled condenser and a constant temperature magnetic stirrer with hot plate. Catalyst was activated by dispersing it with methanol at 40 °C under magnetic stirring. After 1 h of the catalyst activation mustard oil was added to the mixture and then the mixture was vigorously stirred and refluxed at 65 °C for 3 h under stirring at 900 rpm. After the reaction, the catalyst was separated from the biodiesel product by centrifugation and the excessive amount of methanol was evaporated under reduced pressure in a rotary evaporator. The yield of the biodiesel was calculated by using the equation given in the literature [21,22]:

$$\%\ \text{yield} = \frac{\text{Weight of biodiesel produced}}{\text{weight of oil used}} \times 100\%$$

### 2.3. General

The thermal stability of the catalyst was evaluated in a TGA instrument (Perkin Elmer STA 6000) from room-temperature to 890 °C at a ramping rate of 10 °C $min^{-1}$ under a flow of nitrogen. The structures of the samples were examined by means of XRD, SEM, EDX, and FT-IR spectroscopy. The powder X-ray diffractograms of calcined samples were recorded on a Rigaku miniflex diffractometer (Cu-Kα radiation, λ = 1.5406 Å) in 2θ range 10–70 at a scanning rate of 2 °C $min^{-1}$. SEM and EDX were performed on a Jeol, JSM-6290LV instrument. Analysis for components of biodiesel profile determination was performed in GC-MS (Perkin Elmer Claurus 600) equipped with TCD detector and elite wax column. The column temperature was programmed from 60 °C to 220 °C and the rate of increase was 3 °C/min. The carrier gas used for the purpose was helium and the flow rate was maintained at 1 mL/min. IR spectra were recorded in KBr pallets on a Nicolet (Impact 410) FT-IR spectrophotometer. The Brunauer–Emmett–Teller (BET) surface area and pore volume of the prepared catalysts were measured using a Backman Coulter (SA3100) surface area analyzer.

## 3. Results and discussion

### 3.1. Characterizations

#### 3.1.1. Feedstock analysis

The fatty acid compositions according to the manufacturer [22] are given in Table 1 and characteristics of mustard oil used are shown in Table 2 respectively. The acid value was determined according to ASTM D 664 and the water content was determined according to ASTM D 6304-07. It was observed that the acid value and water content of the feedstock were low enough for effective base catalyzed transesterification (water content<299 ppm and acid value<1).

#### 3.1.2. XRD analysis

Fig. 1 depicts the XRD patterns for the shell calcined in the range of 600–700 °C. The spectra were obtained with Cu Kα radiation (λ = 0.15406 nm) at 30 kV, 15 mA in a scan range of 10–70. The

**Table 1**
Fatty acid composition (%) of mustard oil.

| Fatty acid | Structure | Range |
|---|---|---|
| Palmitic | C16:0 | 1–3% |
| Stearic | C18:0 | 0.4–3.5% |
| Arachidic | C20:0 | 0.5–2.4% |
| Behenic | C22:0 | 0.6–2.1% |
| Lignoceric | C24:0 | 0.5–1.1% |
| Oleic | C18:1 | 12–24% |
| Eicosenoic | C20:1 | 3.5–11.6% |
| Erucic | C22:1 | 40–55% |
| Linoleic | C18:2 | 12–16% |
| Linolenic | C18:3 | 7–10% |

**Table 2**
Some physical properties of mustard oil.

| Properties | Mustard oil |
|---|---|
| Acid value (mg KOH $g^{-1}$) | 0.85 |
| Water content (ppm) | 299 |
| Saponification value | 172 |
| Iodine value | 104 |

peaks obtained were compared with the joint committee on powder diffraction standards (JCPDS) file. We considered only four calcination temperatures starting from 600 °C as shell calcined from 100 to 600 °C showed similar XRD patterns. For shell calcined at 600 °C, the main peak was observed at 2θ = 29.47°, 36.37°, 39.48°, 43.55°, 47.87°, 49.05° and 57.89°. These peaks were the characteristic peaks of calcium carbonate corresponding to the JCPDS file no. 85-1108. Peaks of calcium oxide along with some peaks of calcium hydroxide appeared when the shell was calcined at 700 °C. The peaks for calcined shell at 800 and 900 °C appeared at 2θ = 32.14, 37.22, 53.57, 64.24 and 67.49, which were the characteristic peaks for calcium oxide (JCPDS file no. 48-1467). This confirmed the formation of calcium oxide at a calcination temperature of 800 °C [23,24].

### 3.1.3. SEM and EDX analysis

The morphology of the catalyst calcined at different temperatures was observed by SEM (result not shown). It was revealed from the image obtained that the catalyst calcined at 600 °C was not uniform and aggregated rather a clustered kind of arrangement could be observed at the catalyst surface. With higher calcination temperatures it was found that the clustered surface was slowly vanishing and instead the particles of various size and shape were becoming visible.

In order to investigate the effect of calcination temperature on the catalyst surface EDX was also carried out. The EDX analysis revealed that the chemical composition of the catalyst surface was highly influenced at higher calcination temperatures. Table 3 gives the elemental composition of the shells calcined at different temperatures. It is seen from Table 3 that the content of Ca, Na, Mg, Si and Sc are 21.22, 0.37, 1.02, 1.78 and 3.07% (w/w) respectively at 600 °C calcination temperature. The catalyst prepared at 700 °C contains calcium as the main component of the shell along with some traces of scandium, silicon and bromine. Bromine is not detected at 600 °C calcination temperature. It is also seen from Table 3 that calcium (33.43%, w/w) and oxygen (36.34%, w/w) are present at 800–900 °C calcination temperature.

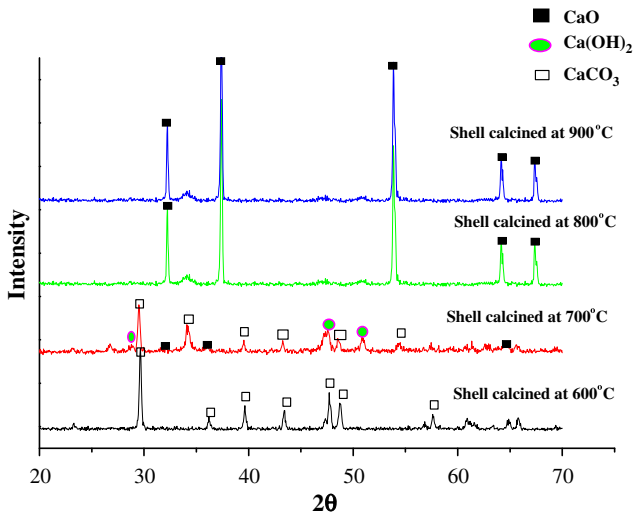


**Fig. 1.** XRD pattern for shell calcined at different temperature.

**Table 3**
EDX analysis of waste shell calcined at different temperatures.

| Shell calcination temperature (°C) | Element | Weight (%) | Atomic (%) |
|---|---|---|---|
| 600 | O | 58.77 | 66.32 |
| | Ca | 21.22 | 9.56 |
| | Sc | 3.07 | 1.23 |
| | Si | 1.78 | 1.15 |
| | Mg | 1.02 | 0.76 |
| | Na | 0.37 | 0.29 |
| 700 | O | 44.84 | 44.59 |
| | Ca | 15.32 | 6.08 |
| | Sc | 2.19 | 0.78 |
| | Si | 0.52 | 0.30 |
| | Br | 0.82 | 0.16 |
| 800 | O | 66.57 | 83.30 |
| | Ca | 33.43 | 16.70 |
| 900 | O | 63.66 | 81.44 |
| | Ca | 36.34 | 18.56 |

### 3.1.4. FTIR analysis

Fig. 2 depicts the FTIR spectra of all the shell calcined at different temperatures along with pure CaO together. It is found that the shell calcined at (a) 600 °C has major absorption band at 1424.29 $cm^{-1}$ which is attributed to the asymmetric stretch for $CO_3^{2-}$ group present in the shell. The other bands for the same sample occur at 873.95 and 711.26 $cm^{-1}$ which represents the out-of-plane band and in-plane band vibration modes respectively of the $CO_3^{2-}$ group. Sharma et al. [25] had also observed the similar band ranges for calcium carbonate present in their study for egg shell. Calcination at higher temperature results into the shifting of the bands to higher energy. This is due to the decrease in the reduced mass of the functional group attached to carbonate ion and consecutively the shell starts to lose carbonate. It is observed from Fig. 4 that upon calcining at 700 °C, a sharp $OH^-$ stretching band also starts to appear at 3644.95 $cm^{-1}$. Calcination at 800 °C temperature indicates that the bands are shifted to higher energy levels. The presence of moisture content was also suggested by Lengyel et al. who observed the band for water around 3600 $cm^{-1}$ [26].

### 3.1.5. TGA–DSC analysis

Comparisons of the TG and DSC measurements for the samples heated at the intermediate rate of 10 °C $min^{-1}$ in nitrogen are depicted in Figs. 3 and 4 respectively. The shell calcined at 600 °C exhibits a single thermal decomposition mass loss beginning at 587.33 °C with a total weight loss of 42.5%. Shell calcined at 700 °C shows two mass losses. The first mass loss in the range of 371.07–434.60 °C is due to the removal of $Ca(OH)_2$ and the second loss in the temperature range 577.78–812.35 °C is attributed to the decomposition of $CaCO_3$ to CaO and $CO_2$ along with some loss of inorganic impurities. This finding in our study has shown similarities with the finding of Lim et al. [27] who reported the evolution of $CO_2$ at a temperature of around 600 °C to around 830 °C. The decomposition of $Ca(OH)_2$ at 500 °C was also reported by Granados et al. [28]. The presence of $Ca(OH)_2$ and formation of CaO in the catalyst at 700 °C are also confirmed by the XRD pattern obtained in our study. The curve obtained also reveals that although the decomposition of $CaCO_3$ starts at around 700 °C, the decomposition is found to be completed at 800 °C. Calcination temperature above 700 °C indicates the formation of one single compound. The decomposition of $CaCO_3$ into CaO and $CO_2$ at high temperature was also reported by some researchers [29,30]. The finding in TGA is also supported by the DSC curve obtained. The DSC curve for shell calcined at 700 °C exhibits an exothermic peak at 424.25 °C which can be attributed to evaporation of water and crystallization and more probable decomposition of organic components or due to possible rearrangement in the structural arrangement within the compound itself. A broad endothermic peak located at the range of 643.26–788.98 °C suggests the

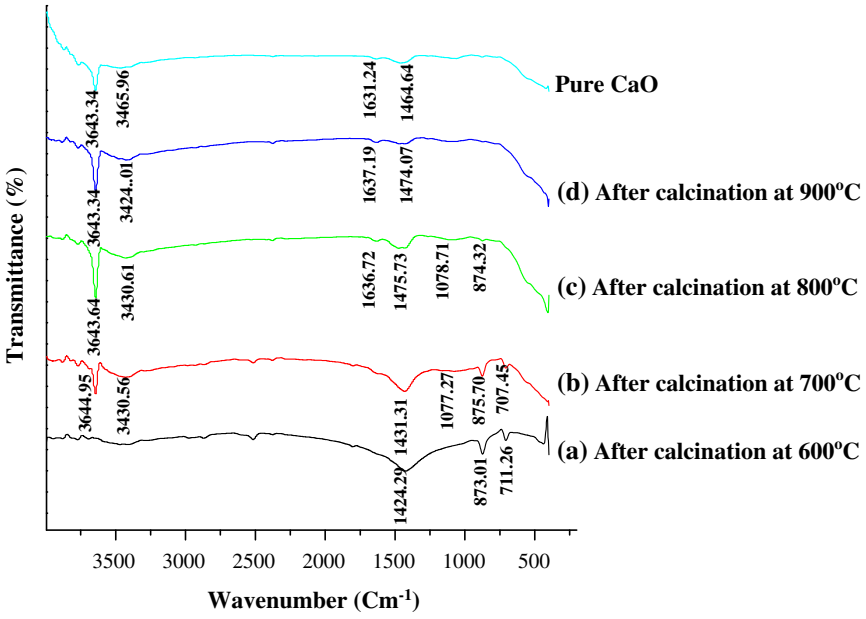


**Fig. 2.** FT-IR pattern for calcined shell and CaO.

decomposition of $CaCO_3$ and possible removal of absorbed water molecules which occurs according to the following dissociation equation [31–33]:

$$CaCO_3(s) \rightarrow CaO(s) + CO_2(g)$$

*3.1.6. Surface and pore volume analysis*

The Brunauer–Emmett–Teller (BET) surface area and the total pore volume of the calcined catalysts are shown in Table 4. It was observed that the shells calcined at 600 °C had total pore volume 0.0128/ $cm^3\ g^{-1}$ and did not show any noticeable BET surface area. For shells calcined in the temperature range 700 °C–900 °C, the BET surface area was between 2.092 and 8.359 $m^2$/g. The increase in BET surface area correlates with the weight loss steps in the TGA curves. For the catalyst calcined at 700 °C, the surface area has increased probably due to a modification of the sample composition during calcination. Further increase in BET surface area for shells calcined above 800 °C, may be caused by the crystal growth of calcium oxide. Calcination of shells at higher temperature also induced an increase of pore volume value which can be attributed to the development of porosity in the calcined shells. The formation of pores in the catalyst prepared was caused by the evolution of gaseous carbonization products ($CO_2$ in our case) and partly due to the formation of CaO.

*3.2. GC analysis of the biodiesel components*

The ester compositions of the biodiesel are given in Table 5 and the GC chromatogram is shown in Fig. 5. Five major peaks were observed in the chromatogram which was identified by comparison with reported data and the profiles from the NIST and Wiley GC-MS libraries. These five main components were identified as octadecanoic acid (2.3%), octadecenoic acid (27.61%), 9,12-octadecadienoic acid (14%), 9,12,15-octadecatrienoic acid (6.9%), and 9-hexadecenoic acid (46.6%).

*3.3. Effect of different parameters*

*3.3.1. Effect of reaction time*

Fig. 6 depicts the reaction time dependence of fatty acid methyl ester (FAME) yield during transesterification by employing *T. striatula* shell derived catalyst. Biodiesel yield is calculated at a regular interval

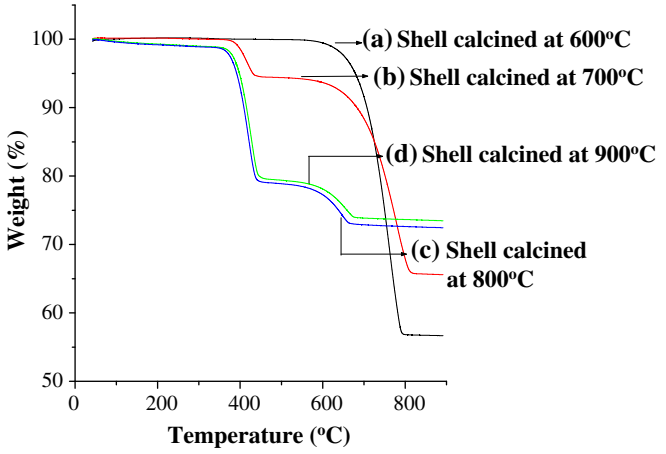


**Fig. 3.** TGA curve of calcined waste shell.

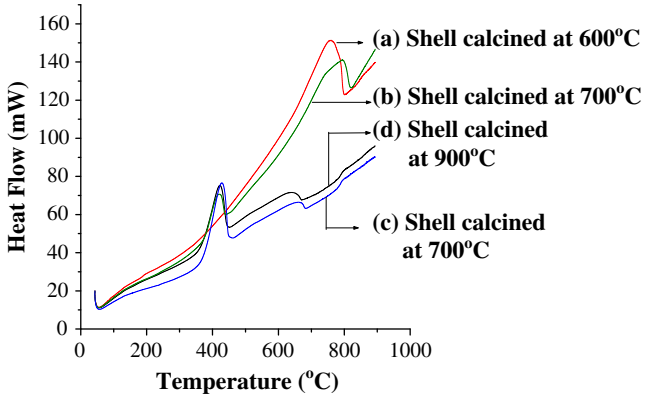


**Fig. 4.** DSC curve of calcined waste shells.

**Table 4**
BET surface area and total pore volume of calcined waste shells of *Turbonilla striatula*.

| | Surface area/$m^2\ g^{-1}$ | Total pore volume/$cm^3\ g^{-1}$ |
|---|---|---|
| Catalyst calcined at 600 °C | – | 0.0128 |
| Catalyst calcined at 700 °C | 2.092 | 0.0153 |
| Catalyst calcined at 800 °C | 4.680 | 0.0507 |
| Catalyst calcined at 900 °C | 8.359 | 0.0571 |

**Table 5**
Fatty acid methyl esters composition of biodiesel synthesized from mustard oil.

| Peak no. | Retention time (min) | Fatty acid methyl esters | Corresponding acid |
|---|---|---|---|
| 1 | 33.24 | Octadecanoic acid | Stearic acid |
| 2 | 39.34 | Octadecenoic acid | Oleic acid |
| 3 | 40.55 | 9,12-Octadecadienoic acid | Linoleic acid |
| 4 | 42.24 | 9,12,15-Octadecatrienoic acid | Linolenic acid |
| 5 | 49.53 | 9-Hexadecenoic acid | Palmitoleic acid |

of 1 h. A good yield of 93.3% and 90.6% is obtained for a reaction time of 6 h by using catalyst calcined at 900 °C and 800 °C respectively. This high yield is attributed to the formation of CaO at the calcination temperatures of 800 °C and 900 °C. The biodiesel yield with the shell calcined at 600 °C after the same interval was found to be very low and a moderate yield was obtained with the shell calcined at 700 °C which is due to the formation of CaO and presence of $Ca(OH)_2$. This explanation may also be supported by the XRD patterns obtained as described in Fig. 1.

*3.3.2. Effect of calcination temperature on transesterification*

To determine the effect of calcination temperature on the activity of the catalyst, the shells were calcined at different temperatures from 100 to 700 °C and then tested for the transesterification of mustard oil. The result shows that the catalyst calcined at temperatures above 700 °C was more active than the shells calcined at 600 °C and 700 °C. Low catalytic activity was observed for catalyst calcined below 700 °C.

*3.3.3. Effect of methanol to oil ratio, temperature and catalyst amount on biodiesel yield*

The effect of methanol to oil molar ratio on biodiesel yield was also investigated. Fig. 7 depicts the FAME yield % with respect to

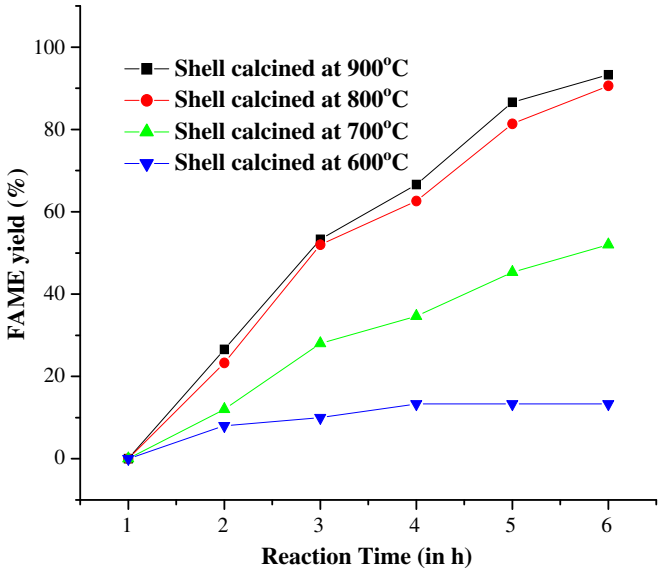


**Fig. 6.** FAME yield with reaction time.

the different methanol to oil molar ratio employed for transesterification. Transesterification was carried out with 3:1, 6:1, 9:1 and 12:1 methanol to oil molar ratio and it was found that the yield increased with increasing methanol to oil ratio. This is due to the formation of methoxy species on the catalyst surface which helps in shifting the reaction towards forward direction. In the present work, the optimum molar ratio is found to be 9:1 over the catalyst.

The FAME yield was also affected by the reaction temperature. An optimum yield of 90% was achieved when the reaction was carried out at $60 \pm 5$ °C and reaction at higher temperature of $70 \pm 5$ °C resulted in decreasing FAME yield which may be due to the loss of methanol at higher temperature. Further the catalyst amount of 3 wt.% was found to be optimum for the reaction. The use of 1.0% and 2% of catalyst concentration rendered biodiesel yield of 66% and 81% respectively. It was observed that when the catalyst concentration was higher than 3%, biodiesel yield remained constant.

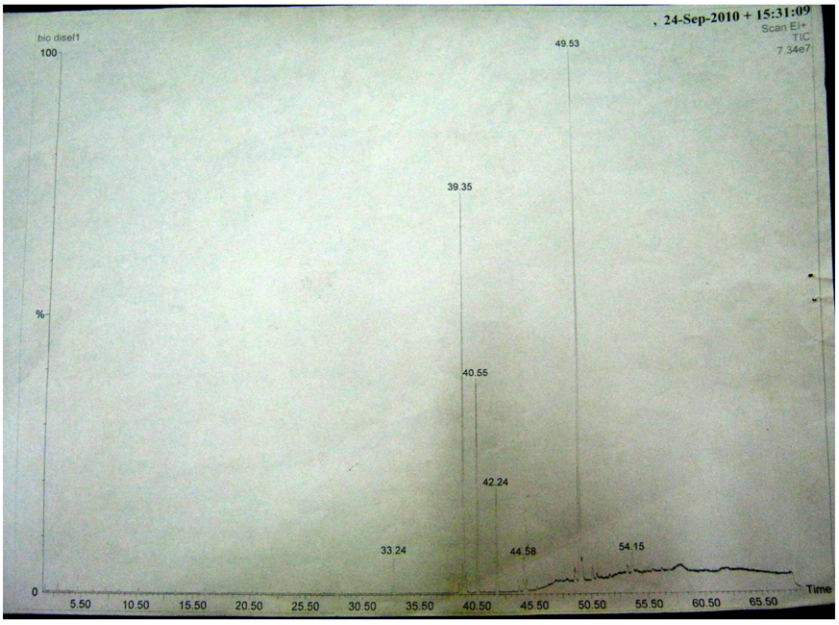


**Fig. 5.** GC-MS chromatogram for biodiesel produced using prepared catalyst.

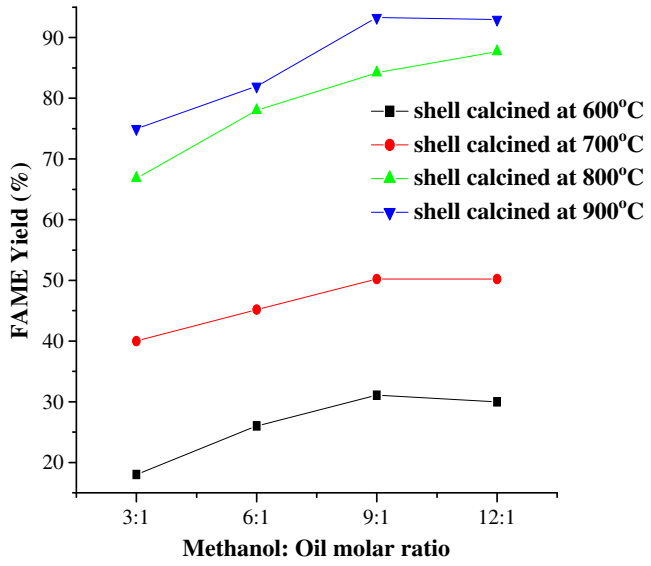


**Fig. 7.** Effect of molar ratio on the yield of biodiesel.

*3.3.4. Reusability of the waste shell derived catalyst*

The reusability of the catalyst prepared at the optimum preparation conditions was investigated by carrying out subsequent reaction cycles. After 6 h of the reaction the catalyst was separated from the reaction mixture by filtration followed by washing with methanol to remove any adsorbed stains. Afterwards it was dried at 120 °C in an oven for 3 h and was used again for second reaction cycle under the same reaction conditions as before. The results are shown in Fig. 8. The results indicated that the yield decreased with the repeated use of the waste shell derived catalysts and it exhibited poor catalytic activity after being used for more than three times. This deactivation was probably due to the structural changes leading to the failure to maintain the form of CaO or its transformation to other form such as $Ca(OH)_2$. This may also be due to the losses of some catalyst amount during the process of washing, filtration and calcination. However, the used catalyst regained its catalytic activity when it was calcined at 900 °C in air for 3 h.

## 4. Conclusion

The waste shell of *T. striatula* was successfully employed for biodiesel production via transesterification. The catalytic activity was found to be related to the calcination temperature as well as to the methanol to oil molar ratio. The shell calcined at 900 °C under the optimum condition of 3.0 wt.% catalyst, 9:1 methanol to oil ratio and a reaction temperature of 65 ± 5 °C exhibited the best catalytic activity when the reaction was carried out for 6 h.

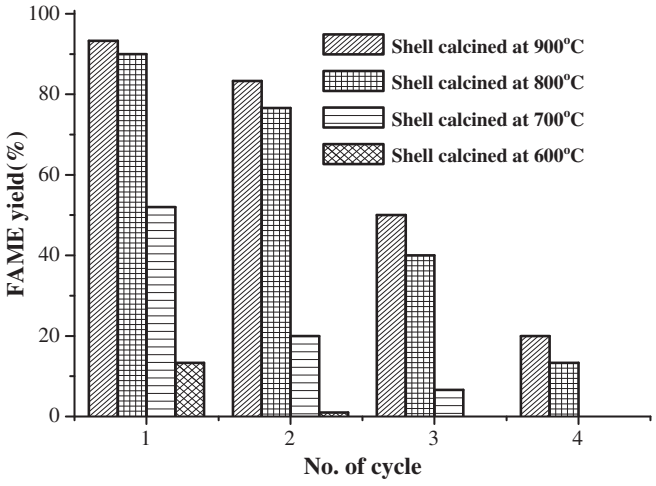


**Fig. 8.** Reusability of the waste shell derived catalyst.

## Acknowledgement

One of the authors, Jutika Boro is highly grateful to the University Grant Commission, Government of India for providing financial assistance in the form of Rajiv Gandhi National Fellowship.

## References

[1] A. Demirbas, Progress and recent trends in biofuels, Progress in Energy and Combustion Science 33 (2007) 1–18.
[2] A.S. Ramadhas, S. Jayaraj, C. Muraleedharan, Biodiesel production from high FFA rubber seed oil, Fuel 84 (2005) 335–340.
[3] S.K. Karmee, A. Chadha, Preparation of biodiesel from crude oil of *Pongamia pinnata*, Bioresource Technology 96 (2005) 1425–1429.
[4] K.J. Harrington, D.V. Catherine, A comparison of conventional and insitu methods of transesterification of seed oil from a series of sunflower cultivars, Journal of the American Oil Chemists' Society 62 (1985) 1009–1013.
[5] A. Shrivastava, R. Prasad, Triglyceride based diesel fuel, Renewable and Sustainable Energy Reviews 4 (2000) 111–133.
[6] K.O. Lim, R.E.H. Sims, Liquid and gaseous biomass fuels, in: R.E.H. Sim (Ed.), Bioenergy options for a cleaner environment—in developed and developing countries, Elsevier Publication, 2004, p. 132.
[7] U. Schuchardt, R. Sercheli, R.M. Vargas, Transesterification of vegetable oils: a review, Journal of the Brazilian Chemical Society 9 (1998) 199–210.
[8] K. Narasimharao, A. Lee, K. Wilson, Catalysts in production of biodiesel: a review, Journal of Biobased Materials and Bioenergy 1 (2007) 19–30.
[9] C. Pinto, L.L.N. Guarieiroa, M.J.C. Rezendea, N.M. Ribeiroa, E.A. Torresb, W.A. Lopesc, P.A. Pereirac, J.B. De, Andrade, Biodiesel: an overview, Journal of the Brazilian Chemical Society 16 (2005) 1313–1330.
[10] A. Demirbas, Biodiesel from triglycerides via transesterification, Biodiesel — A realistic Fuel Alternative for Diesel Engines, Springer, 2007.
[11] Y. Feng, A. Zhang, J. Li, B. He, A continuous process for biodiesel production in a fixed bed reactor packed with cation-exchange resin as heterogeneous catalyst, Bioresource Technology 102 (2011) 3607–3609.
[12] X. Liu, X. Piao, Y. Wang, S. Zhu, Calcium ethoxide as a solid base catalyst for the transesterification of soybean oil to biodiesel, Energy & Fuels 22 (2008) 1313–1317.
[13] A. Kawashima, K. Matsubara, K. Honda, Development of heterogeneous base catalysts for biodiesel production, Bioresource Technology 99 (2008) 3439–3443.
[14] L. Gao, B. Xu, G. Xiao, J. Lv, Transesterification of palm oil with methanol to biodiesel over a KF/hydrotalcite solid catalyst, Energy & Fuels 22 (2008) 3531–3535.
[15] C.M. Garcia, S. Teixeira, L.L. Marciniuk, U. Schuchardt, Transesterification of soybean oil catalyzed by sulfated zirconia, Bioresource Technology 99 (2008) 6608–6613.
[16] A.K. Singh, S.D. Fernando, Transesterification of soybean oil using heterogeneous catalysts, Energy & Fuels 22 (2008) 2067–2069.
[17] A. Alsalme, E.F. Kozhevnikova, I.V. Kozhevnikov, Heteropoly acids as catalysts for liquid-phase esterification and transesterification, Applied Catalysis A: General 349 (2008) 170–176.
[18] O. Ilgen, A.N. Akin, Transesterification of canola oil to biodiesel using MgO loaded with KOH as a heterogeneous catalyst, Energy & Fuels 23 (2009) 1786–1789.
[19] N. Nakatani, H. Takamori, K. Takeda, H. Sakugawa, Transesterification of soybean oil using combusted oyster shell waste as a catalyst, Bioresource Technology 100 (2009) 1510–1513.
[20] Z. Wei, C. Xu, B. Li, Application of waste eggshell as low-cost solid catalyst for biodiesel production, Bioresource Technology 100 (2009) 2883–2885.
[21] D.Y.C. Leung, Y. Guo, Transesterification of neat and used frying oil: optimization for biodiesel production, Fuel Processing Technology 87 (2006) 883–890.
[22] M. Tariq, S. Ali, F. Ahmad, M. Ahmad, M. Zafar, N. Khalid, M.A. Khan, Identification, FT-IR, NMR (1H and 13C) and GC/MS studies of fatty acid methyl esters in biodiesel from rocket seed oil, Fuel Processing Technology 92 (2011) 336–341.
[23] http://www.ksoils.com/whitepapers/whitepaper_mustard_oil_low_heart_risk.pdfaccessed on 14/02/2011.
[24] D. Veilleux, N. Barthelemy, J.C. Trombe, M. Verelst, Synthesis of new apatite phases by spray pyrolysis and their characterization, Journal of Materials Science 36 (2001) 2245–2252.
[25] K. Ming, Y. Guangfu, J.L. Dingming, S. Rong, Synthesis and luminescence properties of red phosphor CaO: $Eu^{3+}$, Journal of Wuhan University of Technology-Materials Science Edition 24 (Feb. 2009) 20–24.
[26] Y.C. Sharma, B. Singh, J. Korstad, Application of an efficient nonconventional heterogeneous catalyst for biodiesel synthesis from *Pongamia pinnata* oil, Energy & Fuels 24 (2010) 3223–3231.
[27] J. Lengyel, Z. Cvengrošová, J. Cvengroš, Transesterification of triacylglycerols over calcium oxide as heterogeneous catalyst, Petroleum & Coal 51 (2009) 216–224.

[28] B.P. Lim, P.G. Maniam, S.A. Hamid, Biodiesel from adsorbed waste oil on spent bleaching clay using CaO as a heterogeneous catalyst, European Journal of Scientific Research 33 (2009) 347–357.
[29] M.L. Granados, M.D.Z. Poves, D.M. Alonso, R. Mariscal, F.C. Galisteo, R.M. Tost, J. Santamaria, J.L.G. Fierro, Biodiesel from sunflower oil by using activated calcium oxide, Applied Catalysis 73 (2007) 317–326.
[30] J.P. Sanders, P.K. Gallagher, Kinetic analyses using simultaneous TG/DSC measurements: part II: decomposition of calcium carbonate having different particle sizes, Journal of Thermal Analysis and Calorimetry 82 (2005) 659–664.
[31] M. Wencka, S.K. Hoffmann, R. Krzyminiewski, S. Mielcarek, Temperature effects in ESR spectra of radical centres in dripstone calcite samples used for ESR dating, Acta Physica Polonica 108 (2005) 491–503.
[32] N.B. Singh, N.P. Singh, Formation of CaO from thermal decomposition of calcium carbonate in the presence of carboxylic acids, Journal of Thermal Analysis and Calorimetry 89 (2005) 159–162.
[33] W. Yong, G. Jiachenga, H. Jinzhua, Z. Yana, Solid reaction mechanism of cahpo4·$2H_2O$ + $CaCO_3$ with and without yttria, Rare Metals 28 (2009) 77–81.